TITLE:

Ambient-pressure organic superconductor κ-(ET)2Ag(CN)[N(CN)2] formed with polymeric silver(I) complex anion

AUTHOR(S):

Yoshida, Yukihiro; Hayama, Hiromi; Ishikawa, Manabu; Otsuka, Akihiro; Yamochi, Hideki; Nakamura, Yuto; Kishida, Hideo; Ito, Hiroshi; Maesato, Mitsuhiko; Saito, Gunzi

CITATION:

Yoshida, Yukihiro ...[et al]. Ambient-pressure organic superconductor κ-(ET)2Ag(CN)[N(CN)2] formed with polymeric silver(I) complex anion. Journal of the Physical Society of Japan 2015, 84: 123801.

ISSUE DATE:

2015-12-15

URL:

http://hdl.handle.net/2433/219409

RIGHT:

© 2015 The Physical Society of Japan.; この論文は出版社版でありません。引用の際には出版社版をご確認ご利用ください。; This is not the published version. Please cite only the published version.

京都大学学術情報リポジトリ
KURENAI 紅
Kyoto University Research Information Repository

京都大学 KYOTO UNIVERSITY
A Self-archived copy in
Kyoto University Research Information Repository
https://repository.kulib.kyoto-u.ac.jp
京都大学学術情報リポジトリ KURENAI 紅 Kyoto University Research Information Repository

Ambient-pressure Organic Superconductor κ-$(ET)_2Ag(CN)[N(CN)_2]$ Formed with Polymeric Silver(I) Complex Anion

Yukihiro Yoshida,[1]* Hiromi Hayama,[1] Manabu Ishikawa,[2] Akihiro Otsuka,[2] Hideki Yamochi,[2] Yuto Nakamura,[3] Hideo Kishida,[3] Hiroshi Ito,[3] Mitsuhiko Maesato,[4] and Gunzi Saito[1,5]

[1]*Faculty of Agriculture, Meijo University, Tempaku-ku, Nagoya 468-8502, Japan*

[2]*Research Center for Low Temperature and Materials Sciences, Kyoto University, Sakyo-ku, Kyoto 606-8501, Japan*

[3]*Department of Applied Physics, Nagoya University, Furo-cho, Chikusa-ku, Nagoya 464-8603, Japan*

[4]*Division of Chemistry, Graduate School of Science, Kyoto University, Sakyo-ku, Kyoto 606-8502, Japan*

[5]*Toyota Physical and Chemical Research Institute, 41-1 Yokomichi, Nagakute, Aichi 480-1192, Japan*

(Received July 22, 2015)

We obtained a new cation radical salt of bis(ethylenedithio)tetrathiafulvalene (ET) with a κ-type packing motif, κ-$(ET)_2Ag(CN)[N(CN)_2]$, by electrooxidation. In the salt, each ET layer is separated by polymeric $\{Ag(CN)[N(CN)_2]^-\}_\infty$ layers, which are composed of Ag(I) ions trigonally coordinated to form an infinite zigzag chain of ~~(~~NC–Ag–NC–Ag~~)~~ with pendant dicyanamides. The salt undergoes a superconducting transition with a midpoint T_c of 6.6 K and an onset T_c of 7.2 K, thereby indicating the highest T_c among ET superconductors formed with a polymeric Ag(I) complex anion.

京都大学 KYOTO UNIVERSITY
A Self-archived copy in
Kyoto University Research Information Repository
https://repository.kulib.kyoto-u.ac.jp
京都大学学術情報リポジトリ KURENAI 紅 Kyoto University Research Information Repository

Molecular cation radical salts of bis(ethylenedithio)tetrathiafulvalene (ET) with a *κ*-type packing motif [Fig. 1(a)] are the most extensively studied molecular system in terms of superconductivity.[1–4] Among them, salts composed of polymeric copper(I) complex anions such as $[Cu(NCS)_2^-]_\infty$,[5] $\{Cu[N(CN)_2]X^-\}_\infty$ (X = Cl[6] and Br[7]), and $\{Cu(CN)[N(CN)_2]^-\}_\infty$,[8,9] are at the core, called "10 K-class superconductors". Because hydrogen atoms of terminal ethylene groups of ET fit into the opening space of the polyanionic layers based on the planar triangular coordination of Cu(I),[10] the structural geometry of the polymeric anions is considered to be the primary cause of the ET packing motif, *i.e.*, the electronic properties of the salt.

In this study, we focus on silver(I), another coinage metal, as the central metal of complex anions. According to the key-keyhole relation described above, it is expected that the larger ion size of Ag(I) (1.29 Å for a six-coordinate system[11]) than that of Cu(I) (0.91 Å for a six-coordinate system[11]) leads to an expanded *κ*-type ET layer while keeping the coordination geometry constant. This, as well as the enhanced electron correlation, should favor the increase in the superconducting critical temperature (T_c) within a BCS-like picture where T_c is controlled by the density of states at the Fermi level ($D(E_F)$).[12] Considering the fact that there is no practical way of applying negative pressure by physical means, except in special cases,[13–15] a chemical modification such as Ag(I) substitution in the 10 K-class superconductors is an obvious target. However, no such materials have been found to date, whereas several ambient-pressure ET superconductors composed of Ag(I) anions, such as polymeric $[Ag(CN)_2^-]_\infty$ (midpoint T_c = 5.0 K)[16] and discrete $Ag(CF_3)_4^-$ (onset T_c = 2.4–11.1 K, depending on the solvent molecules),[17–19] have been reported. Here, we report the synthesis, crystal structure, and electronic properties of a new ambient-pressure superconductor, *κ*-$(ET)_2Ag(CN)[N(CN)_2]$ (*κ*-Ag), composed of polymeric $\{Ag(CN)[N(CN)_2]^-\}_\infty$ anions, which can be regarded as a Ag(I) substitute of *κ*-$(ET)_2Cu(CN)[N(CN)_2]$ (*κ*-Cu)[8,9] with a midpoint T_c = 11.2 K.[20]

Single crystals of *κ*-Ag were obtained by the electrochemical oxidation of ET in an H-shaped cell, which was assembled in a glove box filled with argon gas (H_2O, O_2 < 1 ppm). Typically, ET (0.02 mmol) was added to the anodic compartment, whereas $AgN(CN)_2$ (0.16 mmol) and $(Bu_4N)Ag(CN)_2$ (0.08 mmol) were added to the cathodic compartment. After being dissolved in 18 mL of 1,1,2-trichloroethane/acetonitrile (2:1~5:1 v/v) as much as possible, a constant current (1.0 μA) was passed between the two platinum electrodes over a period of 2 weeks at 20 °C. Black pentagonal or hexagonal block crystals of *κ*-Ag (typical

京都大学 KYOTO UNIVERSITY
A Self-archived copy in
Kyoto University Research Information Repository
https://repository.kulib.kyoto-u.ac.jp
京都大学学術情報リポジトリ KURENAI 紅 Kyoto University Research Information Repository

crystal dimensions: 0.2 × 0.1 × 0.05 mm^3) were harvested together with black square bifrustum crystals of $(ET)Ag_4(CN)_5$[21] and black needle crystals of θ-$(ET)_2Ag_2(CN)[N(CN)_2]_2$,[22] and were separated under a microscope. In addition, many of the chosen crystals were checked for the Raman-active charge-sensitive ν_2 and ν_3 modes prior to physical measurements.

Single-crystal X-ray diffraction experiments were performed on a CCD-type diffractometer (Bruker SMART APEX II) with graphite-monochromated Mo Kα radiation (λ = 0.71073 Å). The κ-Ag salt belongs to the monoclinic system with the space group $P2_1$, as in κ-Cu,[9] over the measured temperature range (100–298 K).[23] Thus, hereafter, we use the crystallographic and band structural data at 100 K, unless otherwise stated. As expected, replacing the Cu(I) ion in κ-Cu with the Ag(I) ion leads to the expansion of the intralayer unit cell area (S) by 1.0%.

Two ET molecules are crystallographically independent, in which the terminal ethylene groups are staggered in one while being eclipsed in the other. The charge on each ET molecule was estimated to be +0.55(7) and +0.50(8) at 298 K and +0.57(5) and +0.59(5) at 100 K on the basis of intramolecular bond lengths.[24] This indicates a uniform charge distribution within the ET layer, *i.e.*, +0.5 for each ET molecule, consistent with the metallic behavior (see below). Raman spectroscopy confirmed this result; the spectrum at room temperature shows a distinct band at 1469 cm^{-1} with a shoulder at 1503 cm^{-1}, which can be readily assigned to charge-sensitive ν_3 and ν_2 modes of $ET^{0.5+}$ species, respectively.[25,26]

As seen in Fig. 1(a), ET molecules are arranged in a κ-type packing motif within the *ab*-plane, and each ET layer is separated by polymeric $\{Ag(CN)[N(CN)_2]^-\}_\infty$ layers. A pair of the two crystallographically independent ET molecules form a dimer with an S = 1/2 spin, which is connected to each other through short C–H···S hydrogen bonds and short heteroatomic S···S contacts within the layer. The center-to-center distances between adjacent dimers in κ-Ag (8.67 Å along the *b*-direction and 7.70 Å along the oblique direction) are longer than those in κ-Cu (8.57 and 7.67 Å).

In the anionic layer, which involves one crystallographically independent $Ag(CN)[N(CN)_2]$ unit, each Ag(I) ion is trigonally coordinated to two cyano groups with no C/N disorder and one dicyanamide as a unidentate ligand through one nitrile nitrogen, to form the infinite zigzag chain of ~~(~~NC–Ag–NC–Ag~~)~~ with pendant dicyanamides along the *b*-axis [Fig. 1(b)]. The Ag(I)–C [2.046(5) Å] and Ag(I)–N [2.408(5) Å] distances are not equal to each other and are comparable to those of an ordered site in κ-(ethylenedithioethylenediselenotetrathiafulvalene)$_2Ag_2(CN)_3$ formed with polymeric

京都大学 KYOTO UNIVERSITY
A Self-archived copy in
Kyoto University Research Information Repository
https://repository.kulib.kyoto-u.ac.jp
京都大学学術情報リポジトリ KURENAI 紅 Kyoto University Research Information Repository

$[Ag_2(CN)_3^-]_\infty$ anions [2.047(7) Å for Ag(I)–C and 2.531(7) Å for Ag(I)–N].[27] In addition, two neighboring ET molecules are coordinated with the Ag(I) ion at the axial sites on the metal center [Ag(I)···S distance: 3.46–3.51 Å], resulting in the distorted trigonal bipyramidal coordination of Ag(I). The geometrical difference of polymeric anions between κ-Ag and κ-Cu is even more marked when the coordination angles are compared: θ_1 = 157.3(2)°, θ_2 = 95.8(2)°, and θ_3 = 106.7(2)° for κ-Ag [Fig. 1(b)] *vs* θ_1 = 138.2(3)°, θ_2 = 101.7(2)°, and θ_3 = 120.2(2)° for κ-Cu [Fig. 1(c)]. The large θ_1 in κ-Ag results in the T-shaped coordination of Ag(I), in contrast to the Y-shaped coordination of Cu(I) in κ-Cu. As seen in Fig. 1(d), one ET molecule (with a dark green hydrogen) in a dimer falls into the opening of the hooklike anionic framework composed of $Ag_3(CN)_2[N(CN)_2]$, whereas the other ET molecule (with a pale green hydrogen) is pinched by multiple adjacent anionic frameworks. These features give firm evidence of the importance of the structural geometry of polymeric anions in determining the packing motif in the ET layers and the electronic state of the salts.

The transfer integrals and band structure of HOMOs of $ET^{0.5+}$ in κ-Ag were calculated using a tight-binding model based on the extended Hückel method.[28] Some band parameters of κ-Ag, together with those of typical κ-$(ET)_2X$ salts, are listed in Table I. As shown in Fig. 2, the band structure clearly shows that the band splits into the upper and lower branches owing to dimerization. The upper energy branch constructs the half-filled band with a bandwidth (W) of 0.544 eV, which is slightly narrower than 0.553 eV of κ-Cu as expected from the expanded lattice. The on-site Coulomb repulsion in an ET dimer (U_d), defined as twice the intradimer transfer energy (t_{b1}) in a dimer model,[29] of κ-Ag (0.482 eV) is slightly smaller than 0.503 eV of κ-Cu. Accordingly, the ratio U_d/W of κ-Ag (0.885) is also slightly smaller than that of κ-Cu (0.909); namely, the lattice expansion indeed leads to the reduced W but not to the enhanced U_d/W. The room-temperature spin susceptibility was roughly estimated to be 6.0×10^{-4} emu mol^{-1} by the average EPR integral intensity (calibrated by $CuSO_4 \cdot 5H_2O$ as a standard) for three single crystals (14–19 μg), which seems to exceed the value of κ-Cu (*ca.* 4.5×10^{-4} emu mol^{-1}).[30] This is possibly associated with the increased $D(E_F)$ as a result of the lattice expansion, although the $D(E_F)$ values estimated on the basis of band calculations are comparable to each other. Note that the t'/t (= $2|t_{b2}|/|t_p + t_q + t_{p'} + t_{q'}|$)[31] of κ-Ag (0.615) is apparently smaller than unity as is the case in κ-Cu (0.643), and that both salts have a two-dimensional (2D)-like transport network. The κ-Ag salt has one-dimensional electron-like and 2D holelike Fermi surfaces along the k_b- and k_a-directions, respectively. There is a tiny gap between the holelike and electron-like Fermi surfaces in the X–M region, as is the case in κ-Cu.

京都大学 KYOTO UNIVERSITY
A Self-archived copy in
Kyoto University Research Information Repository
https://repository.kulib.kyoto-u.ac.jp
京都大学学術情報リポジトリ KURENAI 紅 Kyoto University Research Information Repository

Magnetization data for a set of randomly oriented polycrystals were collected on a Quantum Design MPMS-XL superconducting quantum interference device (SQUID) magnetometer. In an applied magnetic field of 10 Oe, a clear drop in $4\pi\chi$ (χ: magnetic susceptibility), indicating the shielding effect in superconductors, was observed at about 6.5 K in the zero-field cooling (ZFC) process [Fig. 3(a)]. The superconducting volume fractions for four different samples are 15.1, 10.5, 6.8, and 9.2% at 1.9 K. These small but notable values strongly indicate the sign of bulk superconductivity in this salt. Such a drop is not as marked in the field-cooling (FC) process (Meissner effect); the pronounced hysteresis indicates the pinning of the magnetic vortices, and the Meissner ratio χ_{FC}/χ_{ZFC} was estimated to be 0.46 at 1.9 K.

It is known that the superconducting behavior, such as T_c and superconducting volume fraction, of some ET salts varies greatly with the cooling rate of the sample for temperature-dependent measurements.[32,33] We therefore examined the effect of the cooling rate (–10 and –0.2 K min^{-1}) in the range of 10–300 K for one sample, but found that the behavior is almost identical regardless of the cooling rate.

Figure 3(b) shows the temperature dependence of the in-plane resistivity (ρ) of a single crystalline κ-Ag, measured by the conventional four-probe method. As in the case of κ-Cu,[8,20] the κ-Ag salt shows metallic behavior even at room temperature. The room-temperature conductivity σ_{RT} ~ 150 S cm^{-1} is apparently higher than that of κ-Cu (5–50 S cm^{-1}),[8,20] and the temperature dependence shows an upward curvature. On further cooling, the resistivity follows a Fermi-liquid-like T^2 dependence down to *ca.* 20 K and eventually undergoes a sharp drop, indicating that the superconducting transition occurs at about 7 K. The onset (defined as the temperature at which the resistivity starts to deviate from the characteristic curve in normal conduction) and the midpoint (defined as the temperature of the maximum dρ/dT) T_c values were estimated to be 7.2 and 6.6 K, respectively. Note that the T_c values are significantly lower than that of κ-Cu (midpoint T_c = 11.2 K)[20] but higher than that of κ-(ET)$_2$Ag(CN)$_2$·H$_2$O (midpoint T_c = 5.0 K).[16] After the measurements, we confirmed the lattice of the crystal.

The effect of the application of a magnetic field on resistive T_c was investigated to characterize the superconducting state. The measurements were carried out on a Quantum Design PPMS equipped with a rotating stage. The sample orientation to the magnetic field was manually maintained under a microscope to set the magnetic field at 0° to be perpendicular to the *ab*-plane. Because the resistance minimum was observed approximately at 180° in the angular dependence of the magnetoresistance at 6 K in 1 T, the field directions

京都大学 KYOTO UNIVERSITY
A Self-archived copy in
Kyoto University Research Information Repository
https://repository.kulib.kyoto-u.ac.jp
京都大学学術情報リポジトリ KURENAI 紅 Kyoto University Research Information Repository

perpendicular and parallel to the *ab*-plane were determined to be 180(2) and 90(2)°, respectively. As seen in Fig. 4(a), the in-plane T_c monotonically decreases with increasing magnetic field along the *ab*-plane and eventually reaches 3.0 K for the midpoint T_c and 4.1 K for the onset T_c at 9 T. The superconducting transition is noticeably suppressed when the magnetic field is applied perpendicular to the *ab*-plane [Fig. 4(b)]; the transition event was eliminated in magnetic fields higher than 3 T. Note that a resistance hump appears just above the transition only in the case of a magnetic field applied perpendicular to the *ab*-plane [Fig. 4(c)]. This is reminiscent of the behavior shown by some other κ-$(ET)_2X$ salts,[34,35] and the origin will be discussed below.

In Fig. 4(d), the upper critical field (H_{c2}) is plotted versus the temperature in the parallel and perpendicular magnetic fields. The magnetic field that gives a certain midpoint T_c is defined as H_{c2} at $T = T_c$. The Ginzburg–Landau (GL) coherence lengths parallel ($\xi_{\parallel}$) and perpendicular ($\xi_{\perp}$) to the conducting plane correlate with the slope of H_{c2} near T_c as follows:

$$-\mu_0 T_c \left.\frac{dH_{c2\perp}}{dT}\right|_{T=Tc} = \frac{\phi_0}{2\pi\xi_{\parallel}(0)^2} \quad (1)$$

$$-\mu_0 T_c \left.\frac{dH_{c2\parallel}}{dT}\right|_{T=Tc} = \frac{\phi_0}{2\pi\xi_{\parallel}(0)\xi_{\perp}(0)} \quad (2)$$

where μ_0 is the permeability of vacuum and $\phi_0 = h/2e = 2.07 \times 10^{-15}$ Wb is the flux quantum (h: Planck's constant, e: electron charge). $\xi_{\parallel}(0)$ and $\xi_{\perp}(0)$ were estimated to be 20(3) and 1.0(3) nm, respectively, which lead to the high anisotropic parameter $\gamma = \xi_{\parallel}(0)/\xi_{\perp}(0) = 20$, assuming the three-dimensional (3D) GL model.[12] Note that $\xi_{\perp}$ is smaller than the interlayer distance, $d = c\sin\beta = 1.49$ nm. The ratio $\xi_{\perp}(0)/d = 0.67$ indicates that the salt is well described by the Lawrence–Doniach model, which contains the GL model for order parameter variations within the ET layer and couples them through Josephson tunneling.[36] In this case, the resistance hump observed in the mixed (vortex) state in Fig. 4(c) arises primarily from the Josephson coupling of the ET layers along the interlayer direction.

Although all the measured H_{c2} values lie within the Pauli paramagnetic limiting field (H_P) as given by the weak coupling BCS approximation in the absence of spin-orbit scattering, i.e., $H_P = 1.84T_c$ [K] = 12.1 T,[12] $H_{c2\parallel}$ monotonically increases with decreasing temperature in the measured range [Fig. 4(d)]. A similar behavior has been found for other κ-$(ET)_2X$ salts such as X = $Cu(NCS)_2$,[37,38] X = $Cu[N(CN)_2]Br$,[39,40] X = $Cu[N(CN)_2]Cl$,[41] and κ-Cu.[20] The measurements in higher magnetic fields must be a future work to verify the Pauli paramagnetic pair-breaking effect indicating the spin singlet pairing of superconductivity. In this context, the Fulde–Ferrell–Larkin–Ovchinnikov (FFLO) state including Cooper pairs

京都大学 KYOTO UNIVERSITY
A Self-archived copy in
Kyoto University Research Information Repository
https://repository.kulib.kyoto-u.ac.jp
京都大学学術情報リポジトリ KURENAI 紅 Kyoto University Research Information Repository

with nonzero total momentum may survive even above H_P, as in the case of X = $Cu(NCS)_2$.[42,43]

In Fig. 5, we redraw the 3D bar graph showing the T_c values of κ-$(ET)_2X$ with various t'/t and U_d/W values that were reported previously.[44] Data except for those of κ-Ag (**H**) are cited from Ref. 45. In the $t'/t > 0.7$ region, T_c increases as t'/t decreases from unity, changing from T_c = 3.9 K (0.06 GPa) for X = $Cu_2(CN)_3$ (**A**; t'/t = 1.07) to T_c = 12.8 K (0.03 GPa) for X = Cu[$N(CN)_2$]Cl (**C**; t'/t = 0.73), which is associated with the spin fluctuation mechanism of superconductivity. On the other hand, the salts in the $t'/t < 0.7$ region have comparable t'/t values and T_c seems to depend mainly on U_d/W, changing from T_c = 3.6 K for X = I_3 (**G**; U_d/W = 0.81) to T_c = 11.6 K for X = Cu[$N(CN)_2$]Br (**D**; U_d/W = 0.90), which is associated with the electron correlation. The T_c of κ-Ag (**H**) with t'/t = 0.62 and U_d/W = 0.89 can also be explained in the framework of this picture; namely, it is reasonable that the κ-Ag (**H**) with a smaller U_d/W has a lower T_c relative to those of κ-Cu (**E**).

In the present system, the lattice expansion induced by substituting Cu(I) for Ag(I) inevitably led to decreases in both U_d and W, where the U_d of κ-Ag is one of the smallest among the κ-$(ET)_2X$ salts. As seen in Table I, the U_d values of X = $Cu_2(CN)_3$ and κ-Ag with the largest S values are smaller than those of other κ-$(ET)_2X$ salts. Because the structure of polymeric anions plays an important role in the geometry (size and anisotropy) of the ET layers,[10] it is apparent that the small U_d values of X = $Cu_2(CN)_3$ and κ-Ag are closely connected with their anionic structures regardless of the metal ion. κ-Ag is the first Ag(I) substitute of the 10 K-class superconductors composed of polymeric anions, and thus the present work represents an initial step toward future exploration of higher-T_c organic superconductors with metal ions other than Cu(I). In particular, because the change in U_d caused by the lattice expansion would be a distinctive characteristic of dimer-type organic conductors, a future challenge will be to elucidate the relationship between the geometry of the anionic hole and U_d.

In summary, we succeeded in preparing a new ambient-pressure ET superconductor formed with a polymeric Ag(I) complex anion. Because the Ag(I) ion is apparently larger than the Cu(I) ion that has provided a variety of polymeric complex anions yielding 10 K-class ET superconductors, their Ag(I) substitutes are expected to show a higher T_c within a BCS-like model. The present salt indeed expands its crystal lattice compared with the corresponding Cu(I) salt and undergoes a superconducting transition; however, the temperature is lower than that of the Cu(I) salt. According to Fig. 5, this is associated with the fact that the on-target narrower band derived from the expanded crystal lattice did not lead to the enhanced U_d/W

京都大学 KYOTO UNIVERSITY
A Self-archived copy in
Kyoto University Research Information Repository
https://repository.kulib.kyoto-u.ac.jp
京都大学学術情報リポジトリ KURENAI 紅 Kyoto University Research Information Repository

owing to the weakened dimerization. Future works, particularly on the exploration of new κ-$(ET)_2X$ salts formed with other types of polymeric Ag(I) complex anions, are in progress.

Acknowledgment

We thank Dr. Masafumi Sakata (Osaka University) for resistivity measurements at the early stage of this work. Thanks are also due to Drs. Takashi Koretsune (RIKEN) and Yoshiaki Nakano (Kyoto University) for fruitful discussions. This work was supported by JSPS KAKENHI Grant Numbers 23225005 and 26288035.

*E-mail: yyoshida@meijo-u.ac.jp

京都大学 KYOTO UNIVERSITY
A Self-archived copy in
Kyoto University Research Information Repository
https://repository.kulib.kyoto-u.ac.jp
京都大学学術情報リポジトリ KURENAI 紅 Kyoto University Research Information Repository

References

1) T. Ishiguro, K. Yamaji, and G. Saito, *Organic Superconductors* (Springer-Verlag, Berlin, 1998) 2nd ed.
2) T. Mori, H. Mori, and S. Tanaka, Bull. Chem. Soc. Jpn. **72**, 179 (1999).
3) K. Kanoda, J. Phys. Soc. Jpn. **75**, 051007 (2006).
4) G. Saito and Y. Yoshida, Bull. Chem. Soc. Jpn. **80**, 1 (2007).
5) H. Urayama, H. Yamochi, G. Saito, K. Nozawa, T. Sugano, M. Kinoshita, S. Sato, K. Oshima, A. Kawamoto, and J. Tanaka, Chem. Lett. **17**, 55 (1988).
6) J. M. Williams, A. M. Kini, H. H. Wang, K. D. Carlson, U. Geiser, L. K. Montgomery, G. J. Pyrka, D. M. Watkins, J. M. Kommers, S. J. Boryschuk, A. V. Crouch, W. K. Kwok, J. E. Schirber, D. L. Overmyer, D. Jung, and M.-H. Whangbo, Inorg. Chem. **29**, 3272 (1990).
7) M. Kini, U. Geiser, H. H. Wang, K. D. Carlson, J. M. Williams, W. K. Kwok, K. G. Vandervoort, J. E. Thompson, D. L. Stupka, D. Jung, and M.-H. Whangbo, Inorg. Chem. **29**, 2555 (1990).
8) T. Komatsu, T. Nakamura, N. Matsukawa, H. Yamochi, and G. Saito, Solid State Commun. **80**, 843 (1991).
9) H. Yamochi, T. Nakamura, T. Komatsu, N. Matsukawa, T. Inoue, and G. Saito, Solid State Commun. **82**, 101 (1992).
10) H. Yamochi, T. Komatsu, N. Matsukawa, G. Saito, T. Mori, K. Kusunoki, and K. Sakaguchi, J. Am. Chem. Soc. **115**, 11319 (1993).
11) R. D. Shannon, Acta Crystallogr. **A32**, 751 (1976).
12) M. Tinkham, *Introduction to Superconductivity* (McGraw-Hill, New York, 1996) 2nd ed.
13) H. Kusuhara, Y. Sakata, Y. Ueba, K. Tada, M. Kaji, and T. Ishiguro, Solid State Commun. **74**, 251 (1990).
14) T. Yamamoto, R. Kato, H. M. Yamamoto, A. Fukaya, K. Yamasawa, I. Takahashi, H. Akutsu, A. Akutsu-Sato, and P. Day, Rev. Sci. Instrum. **78**, 083906 (2007).
15) H. M. Yamamoto, M. Nakano, M. Suda, Y. Iwasa, M. Kawasaki, and R. Kato, Nat. Commun. **4**, 2379 (2013).
16) H. Mori, I. Hirabayashi, S. Tanaka, T. Mori, and H. Inokuchi, Solid State Commun. **76**, 35 (1990).
17) U. Geiser and J. A. Schlueter, Chem. Rev. **104**, 5203 (2004).
18) J. A. Schlueter, L. Wiehl, H. Park, M. de Souza, M. Lang, H.-J. Koo, and M.-H. Whangbo, J. Am. Chem. Soc. **132**, 16308 (2010).
19) T. Kawamoto, T. Mori, A. Nakao, Y. Murakami, and J. A. Schlueter, J. Phys. Soc. Jpn. **81**, 023705 (2012).
20) T. Nakamura, T. Komatsu, G. Saito, T. Osada, S. Kagoshima, N. Miura, K. Kato, Y. Maruyama, and K. Oshima, J. Phys. Soc. Jpn. **62**, 4373 (1993).
21) U. Geiser, H. H. Wang, L. E. Gerdom, M. A. Firestone, L. M. Sowa, and J. M. Williams, J.

京都大学 KYOTO UNIVERSITY
A Self-archived copy in
Kyoto University Research Information Repository
https://repository.kulib.kyoto-u.ac.jp
京都大学学術情報リポジトリ KURENAI 紅 Kyoto University Research Information Repository

Am. Chem. Soc. **107**, 8305 (1985).

22) Y. Yoshida *et al.*, unpublished data.

23) Crystal data for *κ*-Ag: $C_{23}H_{16}Ag_1N_4S_{16}$, M = 969.33, monoclinic space group $P2_1$, a = 12.764(2) Å, b = 8.653(1) Å, c = 15.981(2) Å, β = 111.673(2)°, V = 1640.2(4) Å^3, Z = 2, T = 100 K, d_{calc} = 1.962 g cm^{-3}, μ(Mo Kα) = 1.661 mm^{-1}, 5451 independent reflections, 397 refined parameters (7 restraints), R_1 = 0.0500 [for $I > 2\sigma(I)$], wR_2 = 0. 1375 (for all data), Flack parameter = 0.03(2), GOF = 1.108. CCDC 1412466. A CIF file is available as a supplemental material.

24) P. Guionneau, C. J. Kepert, G. Bravic, D. Chasseau, M. R. Truter, M. Kurmoo, and P. Day, Synth. Met. **86**, 1973 (1997).

25) H. H. Wang, J. R. Ferraro, J. M. Williams, U. Geiser, and J. A. Schlueter, J. Chem. Soc., Chem. Commun., 1893 (1994).

26) T. Yamamoto, M. Uruichi, K. Yamamoto, K. Yakushi, A. Kawamoto, and H. Taniguchi, J. Phys. Chem. B **109**, 15226 (2005).

27) S. Golhen, L. Ouahab, A. Lebeuze, M. Bouayed, P. Delhaes, Y. Kashimura, R. Kato, L. Binet, and J.-M. Fabre, J. Mater. Chem. **9**, 387 (1999).

28) T. Mori, A. Kobayashi, Y. Sasaki, H. Kobayashi, G. Saito, and H. Inokuchi, Bull. Chem. Soc. Jpn. **57**, 627 (1984). Transfer integrals (t) were estimated by assuming $t = Es$ (E = –10 eV; s: overlap integrals).

29) A. B. Harris and R. V. Lange, Phys. Rev. **157**, 295 (1967).

30) T. Nakamura, T. Nobutoki, T. Takahashi, G. Saito, H. Mori, and T. Mori, J. Phys. Soc. Jpn. **63**, 4110 (1994).

31) M. Tamura, H. Tajima, K. Yakushi, H. Kuroda, A. Kobayashi, R. Kato, and H. Kobayashi, J. Phys. Soc. Jpn. **60**, 3861 (1991). See supplemental material for the intermolecular transfer integrals.

32) A. Kawamoto, K. Miyagawa, and K. Konoda, Phys. Rev. B **55**, 14140 (1997).

33) H. Taniguchi, A. Kawamoto, and K. Konoda, Phys. Rev. B **59**, 8424 (1999).

34) H. Ito, T. Ishiguro, T. Komatsu, G. Saito, and H. Anzai, Physica B **201**, 470 (1994).

35) F. Zuo, J. A. Schlueter, and J. M. Williams, Phys. Rev. B **60**, 574 (1999).

36) W. E. Lawrence and S. Doniach, *Proc. 12th Int. Conf. Low Temp. Phys., Tokyo, 1970*, ed. E. Kanda (Keigaku, Tokyo, 1971).

37) M.-S. Nam, J. A. Symington, J. Singleton, S. J. Blundell, A. Ardavan, J. A. A. J. Perenboom, M. Kurmoo, and P. Day, J. Phys.: Condens. Matter **11**, L477 (1999).

38) F. Zuo, J. S. Brooks, R. H. McKenzie, J. A. Schlueter, and J. M. Williams, Phys. Rev. B **61**, 750 (2000).

39) W. K. Kwok, U. Welp, K. D. Carlson, G. W. Crabtree, K. G. Vandervoort, H. H. Wang, A. M. Kini, J. M. Williams, D. L. Stupka, L. K. Montgomery, and J. E. Thompson, Phys. Rev. B **42**, 8686 (1990).

40) S. Kamiya, Y. Shimojo, M. A. Tanatar, T. Ishiguro, H. Yamochi, and G. Saito, Phys. Rev.

京都大学 KYOTO UNIVERSITY
A Self-archived copy in
Kyoto University Research Information Repository
https://repository.kulib.kyoto-u.ac.jp
京都大学学術情報リポジトリ KURENAI 紅 Kyoto University Research Information Repository

B **65**, 134510 (2002).

41) Y. Shimojo, T. Ishiguro, H. Yamochi, and G. Saito, J. Phys. Soc. Jpn. **71**, 1716 (2002).

42) J. Singleton, J. A. Symington, M.-S. Nam, A. Ardavan, M. Kurmoo, and P. Day, J. Phys.: Condens. Matter **12**, L641 (2000).

43) R. Lortz, Y. Wang, A. Demuer, P. H. M. Böttger, B. Bergk, G. Zwicknagl, Y. Nakazawa, and J. Wosnitza, Phys. Rev. Lett. **99**, 187002 (2007).

44) M. Maesato, Y. Shimizu, T. Ishikawa, G. Saito, K. Miyagawa, and K. Kanoda, J. Phys. IV France **114**, 227 (2004).

45) T. Hiramatsu, Y. Yoshida, G. Saito, A. Otsuka, H. Yamochi, M. Maesato, Y. Shimizu, H. Ito, and H. Kishida, J. Mater. Chem. C **3**, 1378 (2015).

京都大学 KYOTO UNIVERSITY
A Self-archived copy in
Kyoto University Research Information Repository
https://repository.kulib.kyoto-u.ac.jp
京都大学学術情報リポジトリ KURENAI 紅 Kyoto University Research Information Repository

Figure captions

(Color) **Fig. 1.** (a) κ-type packing motif of $ET^{0.5+}$ in κ-$(ET)_2Ag(CN)[N(CN)_2]$ (κ-Ag) at 100 K. Hydrogen atoms are omitted for clarity. A red dotted ellipse shows the $(ET)_2^{\bullet+}$ dimer with an S = 1/2 spin. Calculated transfer integrals (meV) at 100 K (298 K) are t_{b1} = 241 (215), t_{b2} = 84 (81), t_p = –120 (–106), t_q = –12 (–19), $t_{p'}$ = –110 (–99), and $t_{q'}$ = –31 (–32). Anionic chains in (b) κ-Ag and (c) κ-$(ET)_2Cu(CN)[N(CN)_2]$ (κ-Cu). (d) Crystal packing of κ-Ag viewed perpendicular to the anionic layer. The closest hydrogen atom of each ET molecule to the anionic layer is indicated in green (dark green: surrounded by a hooklike anionic framework; pale green: surrounded by multiple anionic frameworks). A gray U-shaped line indicates the opening of the hooklike anionic framework.

(Color) **Fig. 2.** Band dispersion, density of states [$D(E)$ in states eV^{-1} $spin^{-1}$], and Fermi surface of HOMO band of κ-Ag (red) at 100 K, together with those of κ-Cu (black) at 100 K. Energy is given relative to the Fermi energy (E_F).

(Color) **Fig. 3.** Temperature dependence of (a) magnetic susceptibility of randomly oriented polycrystals of κ-Ag in the magnetic field of 10 Oe and (b) resistivity of a single crystal of κ-Ag with the current within the *ab*-plane. Blue closed and open circles in (a) are the zero-field cooling (ZFC) and field cooling (FC) processes, respectively. Inset in (b) is the resistivity data in the whole measured temperature range.

(Color) **Fig. 4.** Variation of T_c for κ-Ag with magnetic field applied (a) parallel and (b) perpendicular to the *ab*-plane. (c) Enlarged figure of (b) to show a resistance hump appearing just above the transition. For the color of each line in (a)–(c), see the corresponding table on the right-hand side in this figure. (d) Upper critical field (H_{c2}) as a function of temperature in an applied magnetic field parallel (red circles) and perpendicular (red triangles) to the *ab*-plane.

(Color) **Fig. 5.** 3D bar graph of T_c versus band parameters t'/t and U_d/W for typical κ-$(ET)_2X$ salts. Band parameters that were calculated based on our crystallographic data at 100 K are cited from Ref. 45 except for those of κ-Ag (red bar). See Table I for letters **A**–**H**.

京都大学 KYOTO UNIVERSITY
A Self-archived copy in
Kyoto University Research Information Repository
https://repository.kulib.kyoto-u.ac.jp
京都大学学術情報リポジトリ KURENAI 紅 Kyoto University Research Information Repository

Table I. Parameters of typical κ-$(ET)_2X$ salts at 100 K.[a]

	X	U_d (eV)	W (eV)	U_d/W	t'/t	S (Å^2)[b]	T_c (K)[c]
A	$Cu_2(CN)_3$	0.483	0.480	1.005	1.074	114.0	3.9 (0.06)
B	$Cu(NCS)_2$	0.520	0.555	0.937	0.803	107.7	10.4
C	$Cu[N(CN)_2]Cl$	0.549	0.607	0.905	0.727	108.4	12.8 (0.03)
D	$Cu[N(CN)_2]Br$	0.531	0.593	0.896	0.672	109.4	11.6
E	$Cu(CN)[N(CN)_2]$ (κ-Cu)	0.503	0.553	0.909	0.643	109.0	11.2
F	$Ag(CN)_2 \cdot H_2O$	0.525	0.584	0.899	0.609	107.7	5.0
G	I_3	0.536	0.660	0.812	0.541	106.5	3.6
H	$Ag(CN)[N(CN)_2]$ (κ-Ag)	0.482	0.544	0.885	0.615	110.4	6.6

[a] X-ray diffraction measurements at 100 K and the extended Hückel band calculations using the obtained data were performed by us. All the data except for those of κ-Ag are cited from Ref. 45. Letters in the leftmost column correspond to those in Fig. 5. [b] Intralayer unit cell area, defined as, for example, the product of lattice parameters a and b for κ-Ag. [c] Values in parentheses are applied pressures (in GPa) that are necessary to realize the maximum T_c.

京都大学 KYOTO UNIVERSITY
A Self-archived copy in
Kyoto University Research Information Repository
https://repository.kulib.kyoto-u.ac.jp
京都大学学術情報リポジトリ KURENAI 紅 Kyoto University Research Information Repository

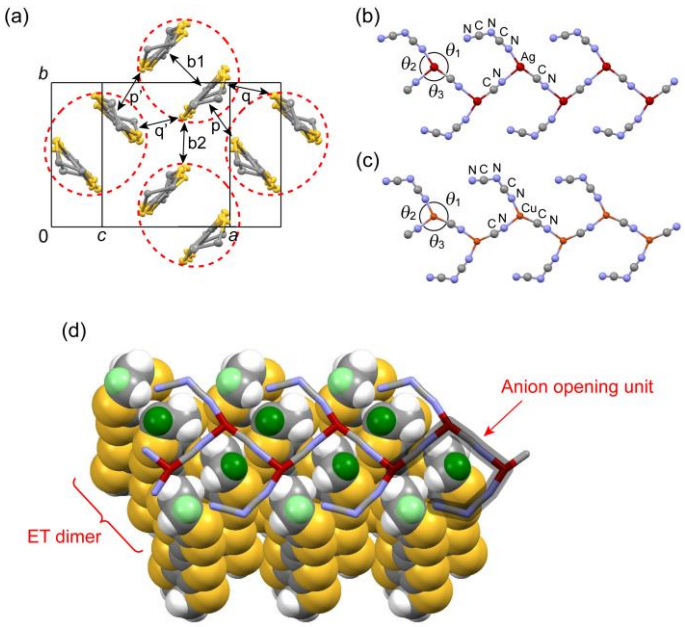

Fig. 1

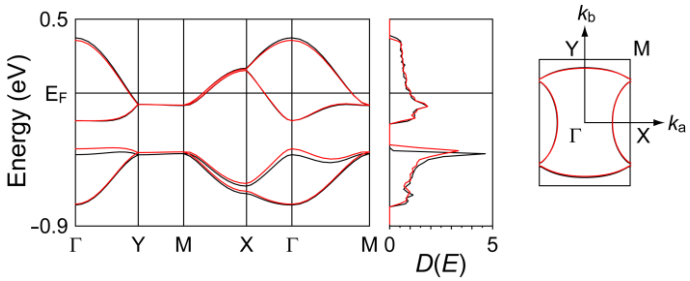

Fig. 2

京都大学 KYOTO UNIVERSITY
A Self-archived copy in
Kyoto University Research Information Repository
https://repository.kulib.kyoto-u.ac.jp
京都大学学術情報リポジトリ KURENAI 紅 Kyoto University Research Information Repository

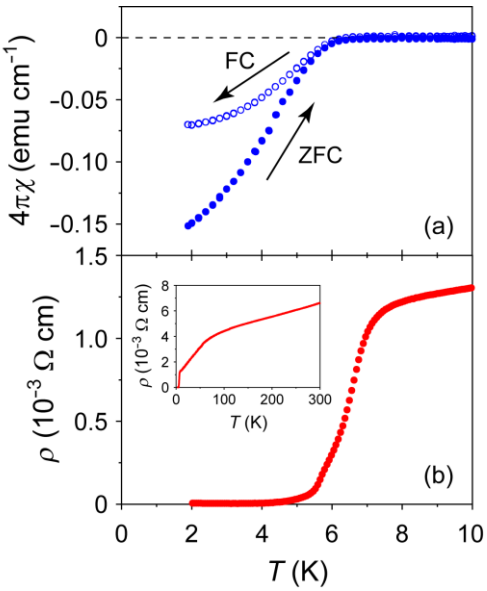

Fig. 3

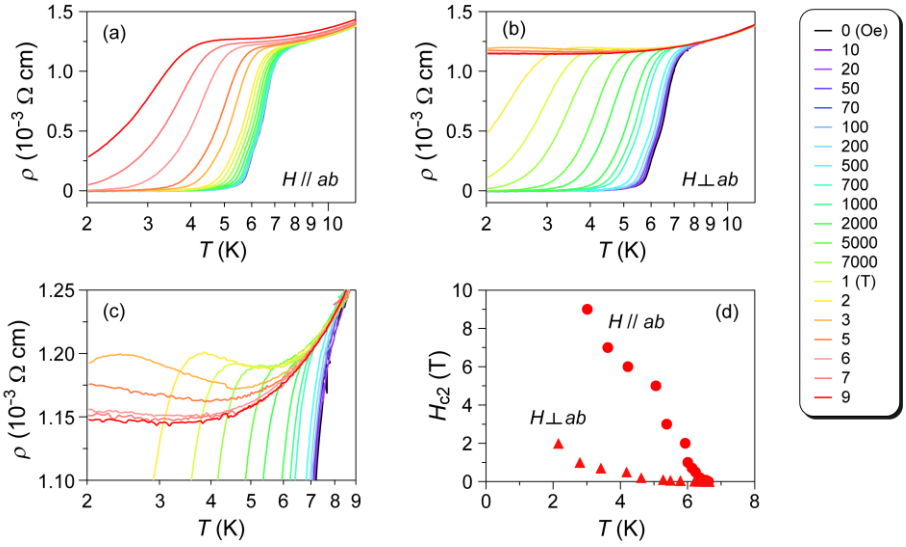

Fig. 4

京都大学 KYOTO UNIVERSITY
A Self-archived copy in
Kyoto University Research Information Repository
https://repository.kulib.kyoto-u.ac.jp
京都大学学術情報リポジトリ KURENAI 紅 Kyoto University Research Information Repository

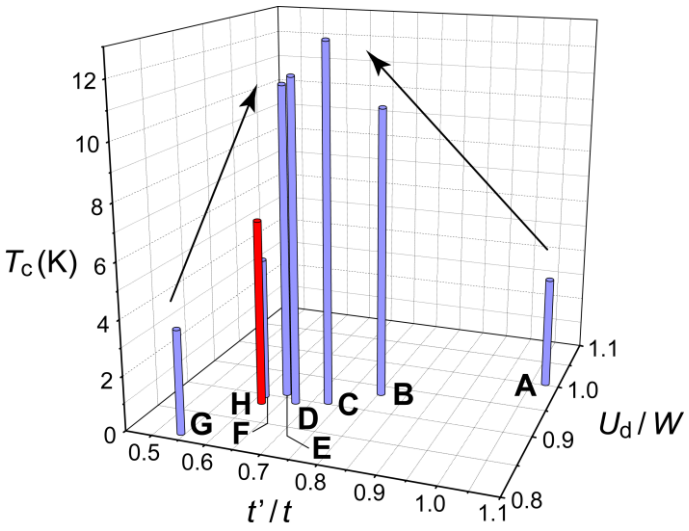

Fig. 5

京都大学 KYOTO UNIVERSITY
A Self-archived copy in
Kyoto University Research Information Repository
https://repository.kulib.kyoto-u.ac.jp
京都大学学術情報リポジトリ KURENAI 紅 Kyoto University Research Information Repository

Supplemental Material

Ambient-pressure Organic Superconductor κ-$(ET)_2Ag(CN)[N(CN)_2]$ Formed with Polymeric Silver(I) Complex Anion

Yukihiro Yoshida, Hiromi Hayama, Manabu Ishikawa, Akihiro Otsuka,

Hideki Yamochi, Yuto Nakamura, Hideo Kishida, Hiroshi Ito,

Mitsuhiko Maesato, and Gunzi Saito

About anisotropy parameter $t'/t = 2|t_{b2}|/|t_p + t_q + t_{p'} + t_{q'}|$ in the text

A program used for the extended Hückel calculations in this study gave the overlap integrals (s) between ET molecules at 100 K:

b1 = –24.08, b2 = –8.37, p = 12.01, q = 1.16, p' = 10.96, q' = 3.08.

Transfer integrals (t) estimated based on the relation $t = ES$ (E = –10 eV) are shown in the caption of Fig. 1. The fact that the b1 value is negative apparently indicates the antibonding interaction between ET molecules within a dimer. Fig. S1 illustrates the orbital phase of the upper HOMO level in this case. It is apparent from this figure that the b2 value is also negative (interaction between lobes of different colors) whereas the remaining p, q, p', and q' are positive (interactions between lobes of the same color). We note that these results are consistent with the calculated overlap integrals shown above.

On the other hand, there is another possible combination of orbital phases, in which the phases in ET dimers A and B remain unchanged whereas those in ET dimers C and D are wholly inversed (Fig. S2). In this case, the intermolecular interaction within ET dimers C and D is still antibonding (b1 < 0), whereas the signs of p, q, p', and q' are inversed due to the antibonding combinations (interactions between lobes of different colors).

Since the p, q, p', and q' values have the same sign in each case, the inter-dimer transfer integral t, defined as the average of those between A–C ($(t_{p'} + t_{q'})/2$) and between A–D ($(t_p + t_q)/2$), can be expressed as

京都大学 KYOTO UNIVERSITY
A Self-archived copy in
Kyoto University Research Information Repository
https://repository.kulib.kyoto-u.ac.jp
京都大学学術情報リポジトリ KURENAI 紅 Kyoto University Research Information Repository

$t = (t_p + t_q + t_{p'} + t_{q'})/4.$

Another inter-dimer transfer integral t' can be expressed as

$t' = t_{b2}/2,$

which leads to the anisotropy parameter t'/t as

$t'/t = 2t_{b2}/(t_p + t_q + t_{p'} + t_{q'}).$

It can be simplified as $t'/t = t_{b2}/(t_p + t_q)$ under the conditions $t_p = t_{p'}$ and $t_q = t_{q'}$. With the aim to focus attention on the absolute value, the above relation can be modified to

$t'/t = 2|t_{b2}|/|t_p + t_q + t_{p'} + t_{q'}|.$

We note that it can also be simplified as $t'/t = |t_{b2}|/|t_p + t_q|$ under conditions $t_p = t_{p'}$ and $t_q = t_{q'}$.

京都大学 KYOTO UNIVERSITY
A Self-archived copy in
Kyoto University Research Information Repository
https://repository.kulib.kyoto-u.ac.jp
京都大学学術情報リポジトリ KURENAI 紅 Kyoto University Research Information Repository

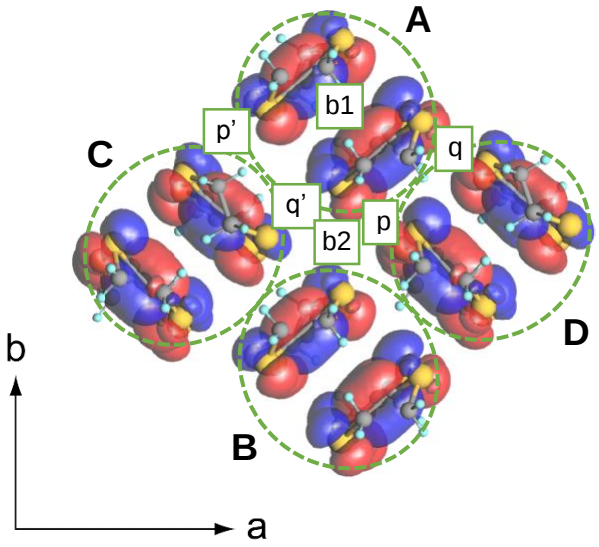

Fig. S1 Schematic of orbital phases in *κ*-Ag used for the extended Hückel calculations. A green dotted ellipse shows the ET dimer (A–D). Calculated overlap integrals at 100 K are b1 = –24.08, b2 = –8.37, p = 12.01, q = 1.16, p' = 10.96, and q' = 3.08×10^{-3}.

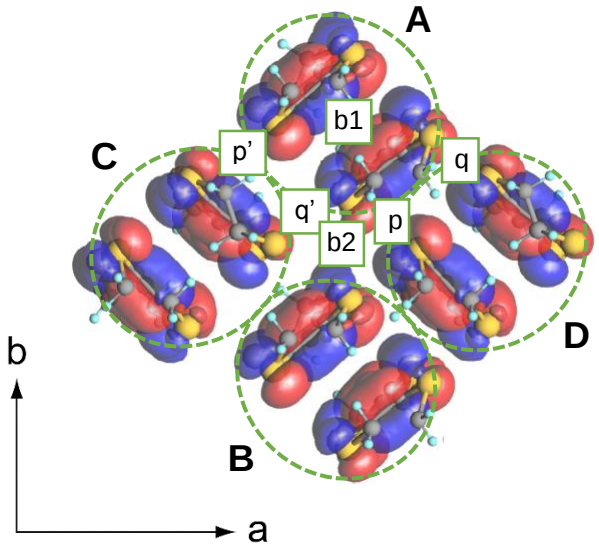

Fig. S2 Schematic of orbital phases, in which the phases in ET dimers C and D are inversed. A green dotted ellipse shows the ET dimer (A–D). In this case, calculated overlap integrals are b1 = –24.08, b2 = –8.37, p = –12.01, q = –1.16, p' = –10.96, and q' = -3.08×10^{-3}.